

PRZEMYSŁAW BORKOWSKI \*

## TECHNIQUE FOR SPATIAL OBJECTS SHAPING WITH ABRASIVE-WATER JET CONTROLLED BY VIRTUAL IMAGE LUMINANCE

The paper presents a novel method for the 3D shaping of different materials using a high-pressure abrasive water jet and a flat target image. For steering the process of movement of the jet, a principle similar to raster image way of record and readout was used. However, respective colors of pixels in such a bitmap are connected with adequate jet feed rate that causes erosion of material with adequate depth. Thanks to that innovation, one can observe spatial imaging of the object. Theoretical basis as well as spatial model of material shaping and experimental stand including steering program are presented in the paper. There are also presented methodic and some experimental erosion results, as well as practical example of object's bas-relief made of metal.

### 1. Introduction

The development of high-pressure abrasive water jet (AWJ) machining method is mainly the result of tool elasticity and the fact that the technique never causes any structural changes in the substrate. Water jets were first used in the 1980s, and since then, much research has been done to optimize the technology [6] and improve the cutting efficiency. Examination of abrasive grain interaction in the treatment zone led to understanding of the mechanism of abrasive erosion [15], making it simpler to characterize and execute specific boring processes [8] such as slender holes [8]. Precision and quality of the treated surfaces were analyzed. Water jet techniques can be applied to ductile materials (e.g., aluminum [12] and titanium [24] alloys), and to assorted brittle materials (e.g., tool steel [22], stone [17, 24] and glass [8,

---

\* *Koszalin University of Technology, Institute of Unconventional HydroJetting Technology, Raclawicka 15-17, 75-620 Koszalin, Poland; E-mail: przemyslaw.borkowski@tu.koszalin.pl*

17]). A number of experiments [14, 20, 22] have clarified the mechanisms of abrasive water jet cutting that define eroded grooves shape [16, 18], process characteristics [19], as prediction of cutting parameters [23]. This knowledge led to simulations of efficiency [21] and cost [23, 25].

As a result of better understanding the cutting mechanism, techniques such as turning [7], milling [8], drilling [9], polishing [13] and surface treatment [1] have become possible. Recently, a new method of automatic abrasive water jet sculpturing [3, 4, 5] of different materials was presented. It enables the production of spatial shaping of an object based on a photograph [2, 10]. In order to manipulate the position of the jet, a principle similar to image rastering was employed. Here, the color of a pixel in the image is correlated to a specific jet feed rate that induces erosion of the substrate to a particular depth [2, 11]. Thanks to this innovation, one can observe spatial imaging of the object.

## 2. Theoretical basis

### 2.1. Principles of shaping material

The concept of spatial material shaping consists in determining, from an image, the light intensity on the surface of a target object. In practice, this process is controlled by a computer navigation program that reads the object's image and then steers the working heads and regulates their feed rates. Its longitudinal movement is velocity-controlled by an analog input, which allows for continuous control of the degree of material removal caused by abrasive water jet.

By referencing the pitting pattern left in the wake of the jet, it is possible to relate the depth of a given cut to the desired pattern in the target image. The amount of time that the jet interacts with the substrate is proportional to the expected erosion depth, and this allows feed rate to be used as the governing parameter for erosion depth (Fig. 1). In this case, the smallest treatable area is determined by the diameter of the jet. The combination of different jet interactions with the substrate allows a spatial bas-relief of the real object to be constructed.

Taking the above conditions into consideration, one can calculate the required interaction time as

$$\Delta t_i = \frac{d_m}{V_i} \quad (1)$$

where  $d_m$  is focusing nozzle diameter while  $V_i$  is velocity of the jet movement above chosen elementary cell (i) of shaped material.

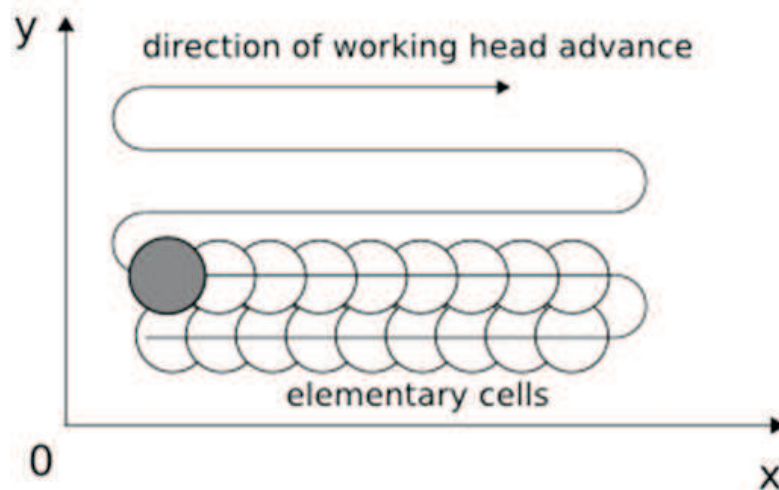


Fig. 1. Concept of image creation

The essence of this method consists in properly specifying the erosion depth and working head positions in relation to the minimum resolution required to capture the target feature. The method relies on image rastering to address each pixel and to construct the whole image. Owing to the similarity between this method and data manipulation of rastered images, the bitmap file format was used as the standard. For such bitmaps, respective pixel colors are correlated to specific erosion depths.

The following steps are required for this technique:

1. The image, typically a photograph, is scanned in gray-scale.
2. The pixel values in the resulting bitmap are converted to working head feed rates that determine the jet interaction time at each location on the substrate.
3. The feed rates are passed to the water jets, and the image geometry is parsed into the control language of a 2-axis plotter that physically rasters the jets across the substrate.

While this approach requires only a simple 2-axis plotter, position control of the jets is crucial, and a specialized program to parse the image data in the control language of the plotter is required.

## 2.2. Photometric basis of object reproduction

Intensity of illumination determines the quality of the resulting image from a photograph. Therefore, special care should be taken when creating the target images because the quality of these images relates directly to the

quality of the product. A basic photometric quantity is energy flux (W) per unit time (t) which is described by

$$\Phi = \frac{\Delta W}{\Delta t} \quad (2)$$

Such a light flux value is calculated by integration of the spectral distribution of energy fluxes that are carried by respective wavelengths of the analyzed radiation as follows:

$$\Phi = K_m \int_{\lambda_1}^{\lambda_2} e(\lambda) \varphi(\lambda) d\lambda, \quad (3)$$

Here,  $K_m$  is a photometric equivalent of radiation, while  $\lambda_1 = 380\text{nm}$  and  $\lambda_2 = 760\text{ nm}$  are wavelengths of visible light,  $e(\lambda)$  is a relative light efficiency of monochromatic radiation and  $\varphi(\lambda)$  is a function of the spectral energy flux distribution for respective wavelengths.

Other important quantities that describe a light source are light intensity and luminance. Light intensity is described by the following formula:

$$I = \frac{\Delta \Phi}{\Delta \omega}, \quad (4)$$

where  $\Delta \omega$  is a block angle relating object surface illumination to the light beam.

The luminance of a luminous surface in a given direction can be expressed as:

$$L = \frac{\Delta I}{\Delta S \cos \varepsilon} = \frac{\Delta \Phi}{\Delta \omega \Delta S \cos \varepsilon} \quad (5)$$

where  $\Delta S$  is surface radiation, while  $\varepsilon$  is the angle between the vector normal to the surface of  $\Delta S$  and the direction of radiation propagation.

Differences in the surface morphology of the target object cause the  $\varepsilon$  angle and luminance of each element to have unique values.

### 2.3. Modeling the spatial shaping process

To a certain extent, the automated method of object quasi-spatial sculpturing based on a target image needs to evaluate the relation between photometric conditions of visible light radiation and jet erosion parameters. Therefore, both radiation and jet dynamics must be modeled.

Considering formulae nos. 5 and 2, one can evaluate the proper exposure time for a given target object. This time value can be used to define the interaction time of the water jet with respect to each feature element of the target object (see formula no. 1). This process can also be expressed via

$$\frac{d_m}{V_i} = K_m \frac{\Delta W}{L_i \Delta \omega \Delta S \cos \varepsilon_i} \quad (6)$$

where  $L_i$  is the luminance of a given element ( $i$ ) taken from the target image, while  $\varepsilon_i$  is the angle between the vector normal to the surface and the direction of radiation propagation.

Imaging the target takes place using perpendicular radiation and perpendicular abrasive-water jet spraying ( $\varepsilon = \varepsilon_i = 0^\circ$ ). Substituting these parameters into (6), one can evaluate the instantaneous velocity of the jet motion above a given element. This is described by the following equation:

$$V_i = \frac{\Delta \omega \Delta S d_m}{K_m \Delta W} L_i, \quad (7)$$

It can be also described in a reduced form which is more useful for analytical purposes:

$$V_i = A L_i, \quad (8)$$

where  $A = \frac{\Delta \omega \Delta S d_m}{K_m \Delta W}$  is a constant involving photometric conditions and characteristics of working head used for AWJ treatment.

Instead of attempting to model full dynamic process control, a simplified model [2] of the direct coupling between feed rate ( $V$ ) and erosion depth ( $h$ ) was applied (Fig. 2). The most universal and precise model is expressed in the form of following power equation:

$$h = b V^{-a}, \quad (9)$$

where  $a$  – is the power exponent, and  $b$  – is an empirical factor.

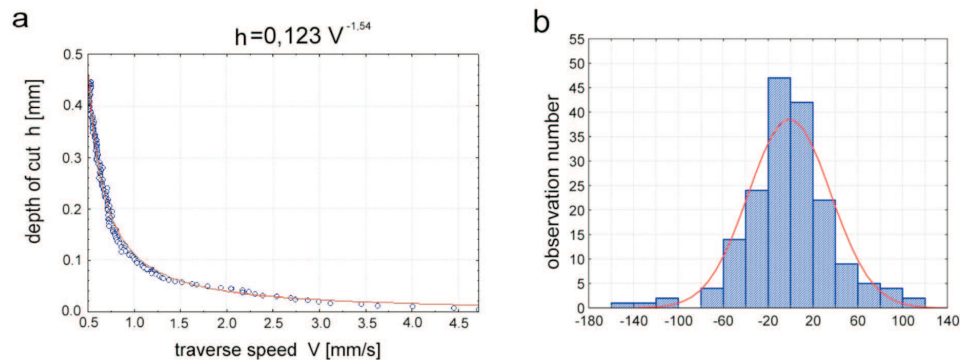


Fig. 2. Experimental results of forming model (a) and exemplary frequency distribution (b)

Based on this analysis, the depth of material erosion is proportional to a negative power function of jet feed rate. This implies that the deepest erosion takes place at minimum jet feed rate, while increasing the feed rate leads to reduced erosion according a nearly hyperbolic dependence. This relation is also suitable for instantaneous values of  $h_i V_i$  related to erosion of a given element.

Substituting equation (8) into (9), one can obtain a new formula to determine the instantaneous values of eroded material:

$$h_i = BL_i^{-a}, \quad (10)$$

where  $B = b \left( \frac{\Delta WK_m}{\Delta \omega \Delta S d_m} \right)^a$  is a new constant involving photometrical and characteristics of the working head.

Analysis of this universal model (10) shows that material erosion depth is proportional to a negative power function of a given elements luminance. In the effect, the most shaded parts of an image correspond with the deepest material erosion, while an increase in luminance leads to a quasi-hyperbolic decrease in erosion depth.

Application of such a model simplifies the raster control method and increases treatment accuracy by enabling the erosion depth to be specified.

### 3. Experimental methodology

#### 3.1. Experimental stand

A special experimental stand was designed and built (see Figs. 3 and 4 for a block diagram and image, respectively). Two stepper-driven lead screws (WX6 08500 by Isert Electronic) were used as linear actuators to control the planar position of the working head, while an additional lead screw system was affixed to these to provide a base for the working head. This gantry ensures XY positioning accuracy of  $\pm 0.005$  mm over a table area of  $1 \text{ m}^2$ . This customized gantry supported a water supply to the working head that was pressurized up to 50 MPa, thereby ensuring constant feed rate of the abrasive material from the reservoir.

Longitudinal movements of the head were produced with stepping frequencies of  $1\text{-}2400 \text{ s}^{-1}$  that taking lead screw travel in account, gives a feed rate of approximately  $0.005\text{-}12 \text{ mm/s}$ , allowing a wide range of different cuts to be made. The actual control of the water jet was controlled with custom-made WaterJetLab software that was written in C++. The FreeDOS platform was used to provide access to PC hardware. This system handles all of the aforementioned functions in only 5000 lines of code, has easily obtainable hardware requirements and presents a simple user interface.

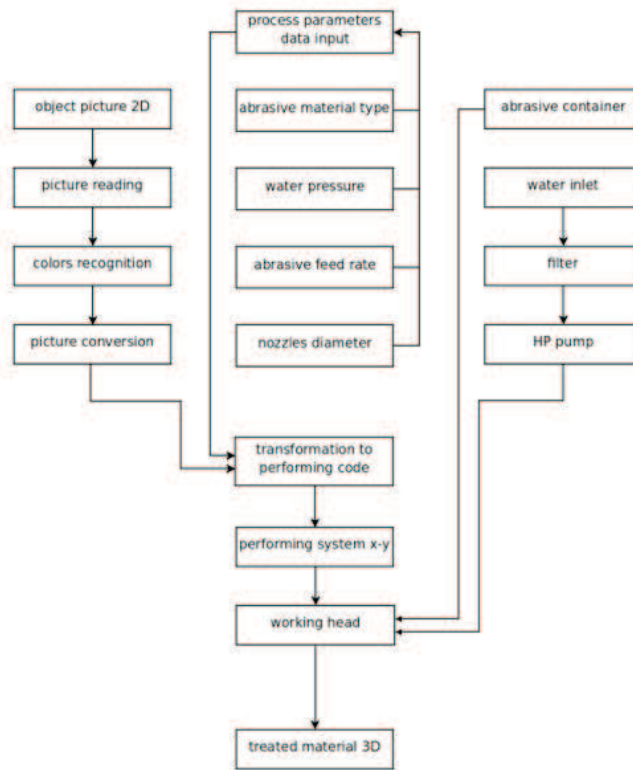


Fig. 3. Detailed structure of experimental stand built



Fig. 4. General view of test stand for spatial material machining with high pressure abrasive-water jet: 1 – frame, 2 – y direction slideways, 3 – x direction slideway, 4 – abrasive-water jet working head, 5 – abrasive feed container, 6 – steering PC computer, 7 – high-pressure water pump type As500/15A

### 3.2. Steering software for sculpturing process realization

Proper function of the system requires the following tasks:

- process configuration prior to running the system,
- principal process control,
- calibration of the sample material's erosive properties with respect to a calibration standard,
- user interface manipulation.

All actions related to process configuration are performed by the user according to a strict procedure [10]. Once prepared, the software records the settings and initializes the appropriate modules. Image processing can be performed by using a filter that transforms bitmaps into 256 step gray scale images based on calculating the luminance from an RGB image according to [3].

$$\text{Grey depth} = 0.3 \cdot \text{Red} + 0.59 \cdot \text{Green} + 0.11 \cdot \text{Blue} \quad (11)$$

The next group of tasks performed by the software pertains to controlling the actual material shaping process. Here, the user's only role is to monitor the process and shut down the system if a problem occurs. A detailed schematic of the x-axis motor control that regulates material erosion is presented in an earlier paper [10]. The system will raster across the sample and determine the appropriate jet parameters based on the gray scale value of each element in relation to that of the subsequent element. This process occurs repeatedly across a line and rasters back (along the y-axis) to the start of the next line.

The calibration phase includes a variety of different water jet parameters designed to regulate the erosion parameters based on a given material. The relevant parameters are the length of individual erosion segments, the number of such segments and the assignation of the proper jet feed rate to individual segments. Another algorithm, which is used for position control, creates a database containing material erosion properties. This serves as the calibration standard for determining erosion depths based on a graphical standard. The last task performed by the software is to handle basic computer services such as graphical display and input for the driving computer.

### 3.3. Research conditions

Different ceramics, glasses, plastics and popular metals served as sample materials. Aluminum alloy, 5mm thick AlMg1SiMn, was used most commonly. Depending upon the shape of the object to be reproduced, the maximum erosion depth defined in the WaterJetLab program was set to values ranging



from 1.5 mm to 2.5 mm. A water nozzle of 0.7 mm diameter and focus nozzle of 2.5 mm diameter was installed in work head, while a standoff distance was set at 5 mm.

Experiments were conducted with a water pressure range of 10-50 MPa, while garnet #80 was used as the abrasive material and was set to output at 0.9 g/s. For such conditions, the dimensions of a mapped gray scale element on sample surface were set to 2x2 mm. Calibration of the material's erosive properties was then conducted. Surface morphology was characterized using a laser gauge (TalySurf CLI 2000 by Taylor Hobson).

#### 4. Abrasive-water jet sculpturing effects

Using this system and approach, basic metal shaping experiments were conducted. Two particular types of test were performed to characterize quality and accuracy and to assess the practicality of the technique.

##### 4.1. Erosion characteristics of different materials

The erosion characteristics of the jet are determined by the physical properties of substrate material. The optimal jet properties such as water pressure, abrasive material type and output, interaction time and the jet spraying angle all depend on the substrate properties. A typical example of this is seen in Fig. 5, which depicts the erosion of AlMg1SiMn under different test conditions. The erosion curves were obtained for popular metals (Fig. 6).

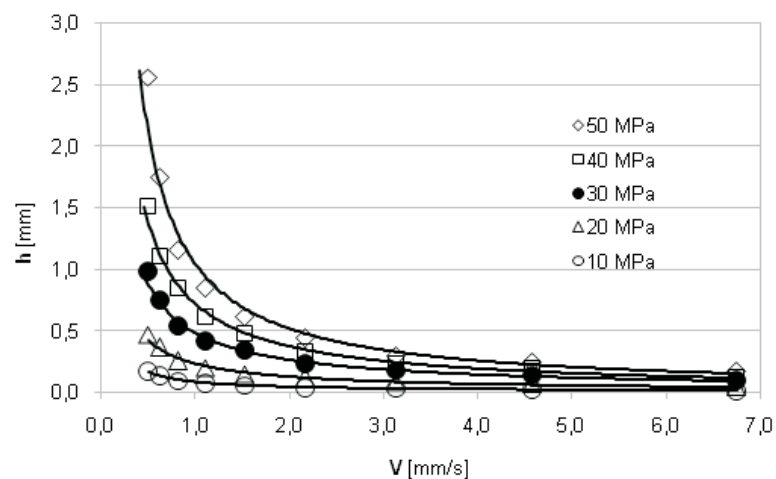


Fig. 5. AlMg1SiMn erosion realized with abrasive-water jet technology (garnet #120,  $m_a=0.90$  g/s)

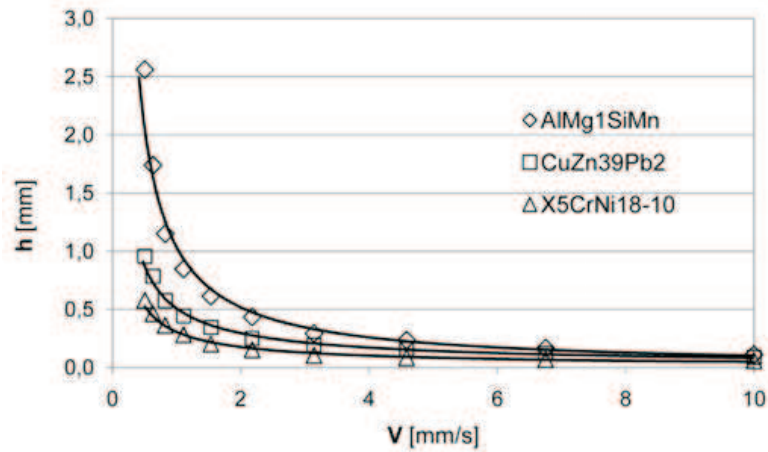


Fig. 6. Metals erosion realized with abrasive-water jet technology ( $p=50$  MPa, garnet #120,  $m_a=0,9$  g/s)

#### 4.2. Surface finish quality

Limiting tests were performed using black and white target image. One should have in mind that during such abrasive water jet spraying, the upper surface of the sample becomes slightly tarnished based on the roughness parameters. Moreover, between the jet paths and at the bottom of the eroded regions are small regions that do not erode. Depending on the erosion parameters, the shape of these regions can form regular edges, as presented in Fig. 7. The shape of these furrows is fairly regular (Fig. 8), and their surface roughness (Fig. 9) is similar to that which occurs during the grinding process.

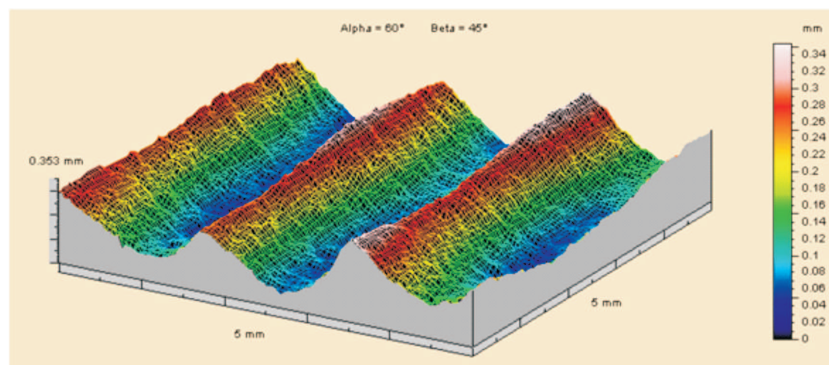


Fig. 7. Shape regularity and edge height of respective jet paths after AWJ treating of AlMg1SiMn ( $p=40$  MPa,  $m_a=0.56$  g/s)

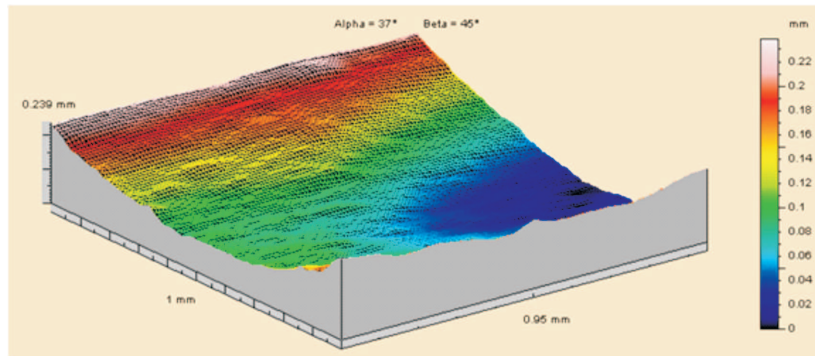


Fig. 8. Typical shape of the bottom of eroded region for AWJ treating of AlMg1SiMn ( $p=40$  MPa,  $m_a=0.56$  g/s)

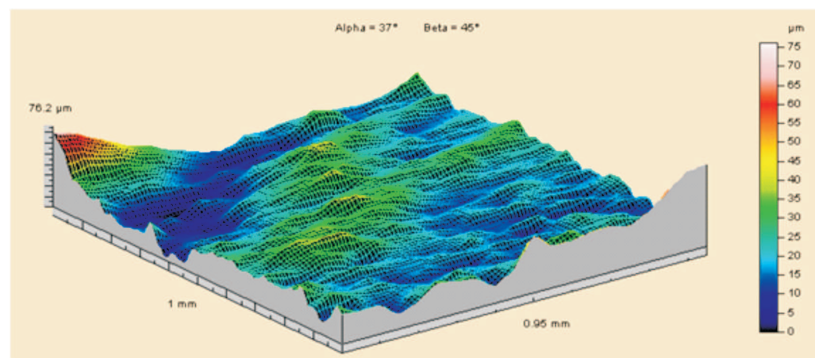


Fig. 9. Quality of the bottom of eroded region for AWJ treating of AlMg1SiMn ( $p=50$  MPa,  $m_a=0.90$  g/s)

### 4.3. Example of practical effects

Basing on this prototype jet-machine, a wide array of different uses for abrasive water jets were considered. Despite the inaccuracies mentioned above, the process needs neither complicated process control nor complex position control. Adequate software of such jet machining processes needs only to ensure the possibility for proper “relocation” between sample material features and abrasive-water jet erosiveness and working head feed rate that is finally responsible for material spatial sculpturing basing on the photo.

Examinations of the effect of material on the ability to produce a particular shape with a high-pressure abrasive-water jet led to the collection of interesting data. Specifically, it was determined that erosion depth can be verified and that spatial objects can be produced based on flat image templates. Common results from such work can be seen in the following picture.

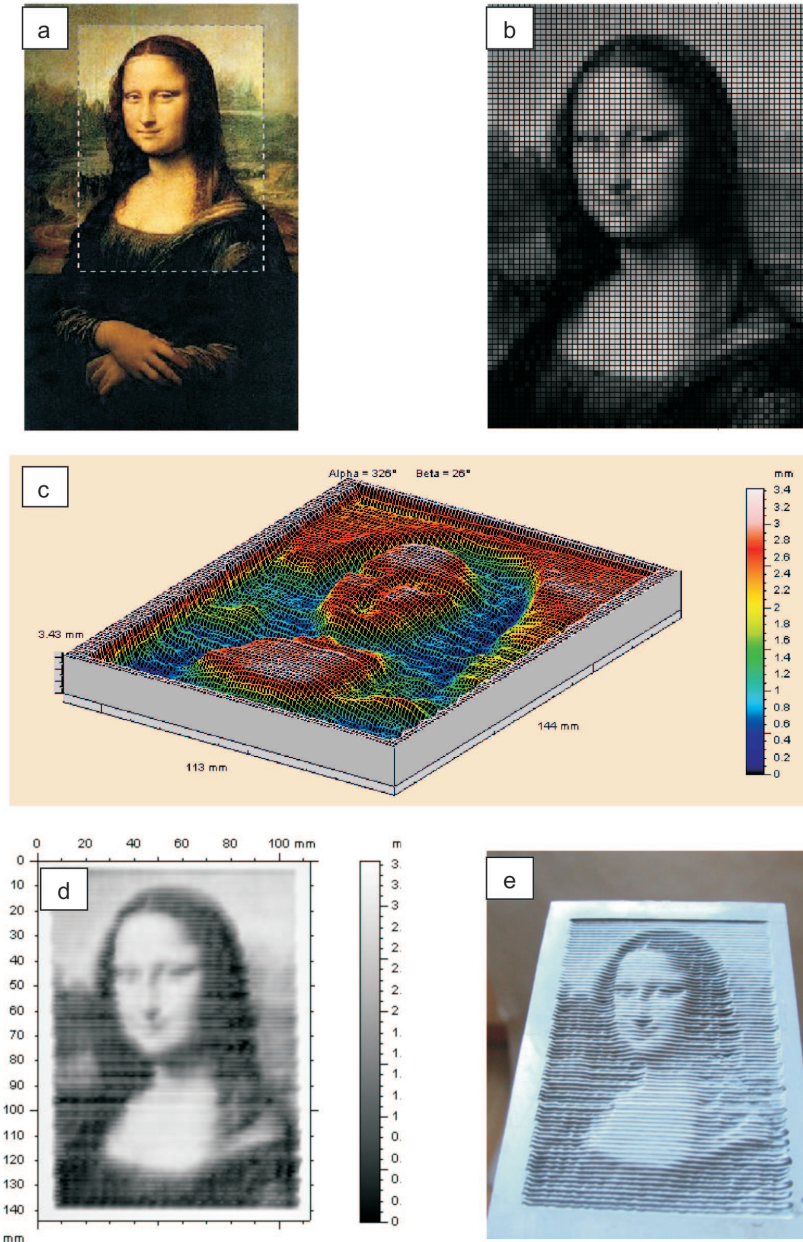


Fig. 10. Images showing important phases of spatial object (Mona Lisa) sculpturing basing on its photocopy: a – picture, b – virtual 2D matrix, c – perspective scanned view showing depth analysis, d – image scanned from the relief, e – photo of 3D bas-relief cut in AlMg1SiMn plate

Fig. 10 presents a photocopy of a well-known painting and includes a set of illustrations showing the important phases of its reproduction in

a metal plate. The presented images show the phases of converting a real object (Fig. a) into a virtual 2D matrix (Fig. b) with the resolution reduced to a level that is reproducible with an abrasive water working head in 3D bass-relief (Fig. c), scanned that way image (Fig. d) and its perspective view showing out its real resolution (Fig. e).

While there is enormous advantage in the automated water jet cutting technique presented, inaccuracy was noted in the form of incomplete reproduction of the erosion depth in regions of high contrast compared to the surroundings. It was observed that proper erosion depth can be achieved only when consecutive pixels in a rastered line share fairly similar gray scale values. Moreover, the quality needs to be improved with respect to the boundary leveling that occurs between individual lines.

It can be stated that, despite the relatively low matrix resolution, the quality of the reproduced image in metal plates is satisfactory. Further, it should be noted that characteristics of the target object are preserved. A particular example of this may be seen in still recognizable subtle smile of La Gioconda. Despite the problem discussed earlier, these results suggest a good future for this technology.

## 5. Conclusions

The abrasive water jet based material shaping technique presented here confirms assumptions about water jet machining and presents a software based procedure for controlling the position of the work head. Based on the presented data, one can generally admit that, despite low matrix resolution, images given in the form of bitmaps were reconstructed relatively well in metal samples. Therefore, the presented method gives satisfactory results.

Manuscript received by Editorial Board, February 23, 2010;  
final version, June 22, 2010.

## REFERENCES

- [1] Borkowski P.: Theoretical and experimental basis of hydro-jet surface treatment. (in polish) ISSN 0239-7129. Koszalin, 2004.
- [2] Borkowski P.: Creation of bas-relief basing on photography using high-pressure abrasive-water jet. *Journal of Machine Engineering*, **8**, 2, 2008, pp.43-51.
- [3] Borkowski P., Szpakowicz A.: Hydro-jetting shaping of bas-relief. *Journal of Machine Engineering*, **13**, 1-2, 2008, pp. 81-89.
- [4] Borkowski P.: Hydrojetting method of bas-relief shaping. *Advances in Manufacturing Science and Technology*. (under review) ACME Ref. No.: 146, 2010.
- [5] Borkowski P., Żukociński T.: Basis of three dimensional material forming using high-pressure abrasive-water jet controlled by virtual image luminance. *Advances in Manufacturing Science and Technology*, **30**, 1, 2006, pp. 53-62.

- [6] Hashish M.: Optimization factors in abrasive-waterjet machining. *Trans. ASME, Journal of Engineering for Industry*. 1991, **113**, 1, pp. 29-37.
- [7] Hashish M.: Turning with abrasive-waterjets – a first investigation. *Trans. ASME, Journal of Engineering for Industry*. 1987, **109**, pp. 281-290.
- [8] Hashish M.: An investigation of milling with abrasive-waterjets. *Trans. ASME, Journal of Engineering for Industry*. 1989, **111**, 2, pp. 158-166.
- [9] Yong Z., Kovacevic R.: Modeling of jetflow drilling with consideration of the chaotic erosion histories of particles. *Wear*. 1997, 209, pp. 284-291.
- [10] Borkowski P., Szpakowicz A.: Abrasive-water jet shaping of bas-relief. 2009 WJTA American Waterjet Conference, August 18-20, 2009, Houston, Texas, Paper No. 3-A.
- [11] Borkowski P., Żukociński T.: Three dimensional method of material forming using high-pressure abrasive-water jet controlled by flat image luminance. 18<sup>th</sup> Int. Conf. Jetting Technology. Gdańsk, 2006, pp. 265-274.
- [12] Chung Y., Geskin E.S., Singh P.J.: Prediction of the geometry of the kerf created in the course of abrasive waterjet machining of ductile materials. 11<sup>th</sup> Int. Conf. on Jet Cutting Technology. St. Andrews, Scotland, 1992, pp. 525-541.
- [13] Fenggang L., Geskin E. S., Tismenetskiy L.: Feasibility study of abrasive waterjet polishing. 13<sup>th</sup> Int. Conf. on Jetting Technology. Sardinia, 1996, pp. 709-723.
- [14] Gropetti R., Gutema T., Di Lucchio A.: A Contribution to the analysis of some kerf quality attributes for precision abrasive water jet cutting. 14<sup>th</sup> Int. Conf. on Jetting Technology. Brugge, 1998, pp. 253-269.
- [15] Hashish M.: On the modeling of abrasive-waterjet cutting. 7<sup>th</sup> Int. Symposium. on Jet Cutting Technology. Ottawa, Canada, 1984. Paper E1, pp. 249-265.
- [16] Henning A., Westkamper E.: Modelling of contour generation in abrasive waterjet cutting. 15<sup>th</sup> Int. Conf. on Jetting Technology. Ronneby, 2000, pp. 309-320.
- [17] Lauand V.H., Hennies W.T., Stellan A. Jr.: Glass and marble (Cachoeiro de Itapemirim) milling with abrasive water jetting. 19<sup>th</sup> Int. Conference Water Jetting. BHR Group. Nottingham, 2008, pp. 121-139.
- [18] Laurinat A., Louis H., Meier-Wiechert G.: A model for milling with abrasive water jets. 7<sup>th</sup> American Water Jet Conf. Seattle, Washington, 1993. Paper 8, pp. 119-139.
- [19] Momber A.W.: A generalized abrasive water jet model. 8<sup>th</sup> American Water Jet Conf. Houston, Texas, 1995. Paper 25, pp. 359-376.
- [20] Tan D.K.M.: A model for the surface finish in abrasive-waterjet cutting. 8<sup>th</sup> Int. Symposium. on Jet Cutting Technology. Durham, England, 1986. Paper 31, pp. 309-313.
- [21] Yong Z., Kovacevic R.: 3D simulation of macro and micro characteristics for AWJ machining. 9<sup>th</sup> American Water Jet Conf. Dearborn, Michigan, 1997. Paper 9, pp. 133-144.
- [22] Zeng J., Kim T.J.: Development of an abrasive waterjet kerf cutting model for brittle materials. 11<sup>th</sup> Int. Conf. on Jet Cutting Technology. St. Andrews, Scotland, 1992, pp. 483-501.
- [23] Zeng J., Kim T.J.: Parameter prediction and cost analysis in abrasive waterjet cutting operations. 7<sup>th</sup> American Water Jet Conf. Seattle, Washington, 1993, Paper 11, pp. 175-189.
- [24] Zhang S., Galecki G., Summers D.A., Swallow C.: Use of pre-profiling a milled pocket as a means of improving machining and lowering energy costs. 2007 WJTA Conference and Expo. Houston, Texas, 2007. Paper 3-H.
- [25] Zhang S., Shepherd J.D., Summers D.A.: Experimental investigation of rectangular pocket milling with abrasive water jet using specially designed tool. 17<sup>th</sup> International Conference on Water Jetting. BHR Group. Mainz, Germany, 2004, pp. 435-447.

**Technika przestrzennego kształtowania przedmiotów strugą wodno-ścierną sterowaną luminancją wirtualnego obrazu****Streszczenie**

W artykule przedstawiono nową metodę przestrzennego kształtowania powierzchni przedmiotów z różnych materiałów przy użyciu wysokociśnieniowej strugi wodno-ścierniej. Umożliwia ona automatyczne wykonywanie płaskorzeźby obiektu na podstawie jego obrazu. Ogólna koncepcja tej metody polega na wierszującym erodowaniu materiału przez wysokociśnieniową strugę wodno-ścierną przemieszczającą się z odpowiednio zróżnicowaną prędkością. Umożliwia to sterowanie czasem oddziaływania strugi na materiał obrabiany, dzięki czemu uzyskuje się analogiczne zróżnicowanie głębokości erozji. Wykorzystując do tego zróżnicowane natężenie oświetlenia obiektu, zarejestrowane na jego fotograficznym obrazie można odtworzyć jego przestrzenne ukształtowanie. Dzięki procedurze takiego selektywnego pozycjonowania głowicy roboczej wytwarzającej strugę wodno-ścierną o odpowiednich właściwościach nacina się w obrabianym materiale poszczególne ścieżki poobróbkowe, które umieszczone obok siebie tworzą płaskorzeźbę wirtualnego obrazu. W artykule tym omówiono stanowisko badawcze zbudowane do realizacji takiej metody wykonywania płaskorzeźb oraz metodykę i warunki przestrzennego kształtowania różnych materiałów. Zaprezentowano także rezultaty przeprowadzonych badań wraz z analizą jakości uzyskiwanych powierzchni a także zademonstrowano jeden z przykładowych obiektów wyrzeźbionych tą metodą w próbce stopu aluminium.